

Search for a muonic dark force at BABAR

J. P. Lees,¹ V. Poireau,¹ V. Tisserand,¹ E. Grauges,² A. Palano,³ G. Eigen,⁴ D. N. Brown,⁵ Yu. G. Kolomensky,⁵ H. Koch,⁶ T. Schroeder,⁶ C. Hearty,⁷ T. S. Mattison,⁷ J. A. McKenna,⁷ R. Y. So,⁷ V. E. Blinov,^{8a,8b,8c} A. R. Buzykaev,^{8a} V. P. Druzhinin,^{8a,8b} V. B. Golubev,^{8a,8b} E. A. Kravchenko,^{8a,8b} A. P. Onuchin,^{8a,8b,8c} S. I. Serednyakov,^{8a,8b} Yu. I. Skovpen,^{8a,8b} E. P. Solodov,^{8a,8b} K. Yu. Todyshev,^{8a,8b} A. J. Lankford,⁹ J. W. Gary,¹⁰ O. Long,¹⁰ A. M. Eisner,¹¹ W. S. Lockman,¹¹ W. Panduro Vazquez,¹¹ D. S. Chao,¹² C. H. Cheng,¹² B. Echenard,¹² K. T. Flood,¹² D. G. Hitlin,¹² J. Kim,¹² T. S. Miyashita,¹² P. Ongmongkolkul,¹² F. C. Porter,¹² M. Röhrken,¹² Z. Huard,¹³ B. T. Meadows,¹³ B. G. Pushpawela,¹³ M. D. Sokoloff,¹³ L. Sun,^{13,*} J. G. Smith,¹⁴ S. R. Wagner,¹⁴ D. Bernard,¹⁵ M. Verderi,¹⁵ D. Bettoni,^{16a} C. Bozzi,^{16a} R. Calabrese,^{16a,16b} G. Cibinetto,^{16a,16b} E. Fioravanti,^{16a,16b} I. Garzia,^{16a,16b} E. Luppi,^{16a,16b} V. Santoro,^{16a} A. Calcaterra,¹⁷ R. de Sangro,¹⁷ G. Finocchiaro,¹⁷ S. Martellotti,¹⁷ P. Patteri,¹⁷ I. M. Peruzzi,¹⁷ M. Piccolo,¹⁷ A. Zallo,¹⁷ S. Passaggio,¹⁸ C. Patrignani,^{18,†} B. Bhuyan,¹⁹ U. Mallik,²⁰ C. Chen,²¹ J. Cochran,²¹ S. Prell,²¹ H. Ahmed,²² A. V. Gritsan,²³ N. Arnaud,²⁴ M. Davier,²⁴ F. Le Diberder,²⁴ A. M. Lutz,²⁴ G. Wormser,²⁴ D. J. Lange,²⁵ D. M. Wright,²⁵ J. P. Coleman,²⁶ E. Gabathuler,²⁶ D. E. Hutchcroft,²⁶ D. J. Payne,²⁶ C. Touramanis,²⁶ A. J. Bevan,²⁷ F. Di Lodovico,²⁷ R. Sacco,²⁷ G. Cowan,²⁸ Sw. Banerjee,²⁹ D. N. Brown,²⁹ C. L. Davis,²⁹ A. G. Denig,³⁰ M. Fritsch,³⁰ W. Gradl,³⁰ K. Griessinger,³⁰ A. Hafner,³⁰ K. R. Schubert,³⁰ R. J. Barlow,^{31,‡} G. D. Lafferty,³¹ R. Cenci,³² A. Jawahery,³² D. A. Roberts,³² R. Cowan,³³ R. Cheaib,³⁴ S. H. Robertson,³⁴ B. Dey,^{35a} N. Neri,^{35a} F. Palombo,^{35a,35b} L. Cremaldi,³⁶ R. Godang,^{36,§} D. J. Summers,³⁶ P. Taras,³⁷ G. De Nardo,³⁸ C. Sciacca,³⁸ G. Raven,³⁹ C. P. Jessop,⁴⁰ J. M. LoSecco,⁴⁰ K. Honscheid,⁴¹ R. Kass,⁴¹ A. Gaz,^{42a} M. Margoni,^{42a,42b} M. Posocco,^{42a} M. Rotondo,^{42a} G. Simi,^{42a,42b} F. Simonetto,^{42a,42b} R. Stroili,^{42a,42b} S. Akar,⁴³ E. Ben-Haim,⁴³ M. Bomben,⁴³ G. R. Bonneaud,⁴³ G. Calderini,⁴³ J. Chauveau,⁴³ G. Marchiori,⁴³ J. Ocariz,⁴³ M. Biasini,^{44a,44b} E. Manoni,^{44a} A. Rossi,^{44a} G. Batignani,^{45a,45b} S. Bettarini,^{45a,45b} M. Carpinelli,^{45a,45b,¶} G. Casarosa,^{45a,45b} M. Chrzaszcz,^{45a} F. Forti,^{45a,45b} M. A. Giorgi,^{45a,45b} A. Lusiani,^{45a,45c} B. Oberhof,^{45a,45b} E. Paoloni,^{45a,45b} M. Rama,^{45a} G. Rizzo,^{45a,45b} J. J. Walsh,^{45a} A. J. S. Smith,⁴⁶ F. Anulli,^{47a} R. Faccini,^{47a,47b} F. Ferrarotto,^{47a} F. Ferroni,^{47a,47b} A. Pilloni,^{47a,47b} G. Piredda,^{47a} C. Büniger,⁴⁸ S. Dittrich,⁴⁸ O. Grünberg,⁴⁸ M. Heß,⁴⁸ T. Leddig,⁴⁸ C. Voß,⁴⁸ R. Waldi,⁴⁸ T. Adye,⁴⁹ F. F. Wilson,⁴⁹ S. Emery,⁵⁰ G. Vasseur,⁵⁰ D. Aston,⁵¹ C. Cartaro,⁵¹ M. R. Convery,⁵¹ J. Dorfan,⁵¹ W. Dunwoodie,⁵¹ M. Ebert,⁵¹ R. C. Field,⁵¹ B. G. Fulsom,⁵¹ M. T. Graham,⁵¹ C. Hast,⁵¹ W. R. Innes,⁵¹ P. Kim,⁵¹ D. W. G. S. Leith,⁵¹ S. Luitz,⁵¹ V. Luth,⁵¹ D. B. MacFarlane,⁵¹ D. R. Muller,⁵¹ H. Neal,⁵¹ B. N. Ratcliff,⁵¹ A. Roodman,⁵¹ M. K. Sullivan,⁵¹ J. Va'vra,⁵¹ W. J. Wisniewski,⁵¹ M. V. Purohit,⁵² J. R. Wilson,⁵² A. Randle-Conde,⁵³ S. J. Sekula,⁵³ M. Bellis,⁵⁴ P. R. Burchat,⁵⁴ E. M. T. Puccio,⁵⁴ M. S. Alam,⁵⁵ J. A. Ernst,⁵⁵ R. Gorodeisky,⁵⁶ N. Guttman,⁵⁶ D. R. Peimer,⁵⁶ A. Soffer,⁵⁶ S. M. Spanier,⁵⁷ J. L. Ritchie,⁵⁸ R. F. Schwitters,⁵⁸ J. M. Izen,⁵⁹ X. C. Lou,⁵⁹ F. Bianchi,^{60a,60b} F. De Mori,^{60a,60b} A. Filippi,^{60a} D. Gamba,^{60a,60b} L. Lancieri,⁶¹ L. Vitale,⁶¹ F. Martinez-Vidal,⁶² A. Oyanguren,⁶² J. Albert,⁶³ A. Beaulieu,⁶³ F. U. Bernlochner,⁶³ G. J. King,⁶³ R. Kowalewski,⁶³ T. Lueck,⁶³ I. M. Nugent,⁶³ J. M. Roney,⁶³ B. Shuve,⁶³ N. Tasneem,⁶³ T. J. Gershon,⁶⁴ P. F. Harrison,⁶⁴ T. E. Latham,⁶⁴ R. Prepost,⁶⁵ and S. L. Wu⁶⁵

(BABAR Collaboration)

¹Laboratoire d'Annecy-le-Vieux de Physique des Particules (LAPP), Université de Savoie, CNRS/IN2P3, F-74941 Annecy-Le-Vieux, France

²Universitat de Barcelona, Facultat de Física, Departament ECM, E-08028 Barcelona, Spain

³INFN Sezione di Bari and Dipartimento di Fisica, Università di Bari, I-70126 Bari, Italy

⁴University of Bergen, Institute of Physics, N-5007 Bergen, Norway

⁵Lawrence Berkeley National Laboratory and University of California, Berkeley, California 94720, USA

⁶Ruhr Universität Bochum, Institut für Experimentalphysik I, D-44780 Bochum, Germany

⁷University of British Columbia, Vancouver, British Columbia, Canada V6T 1Z1

^{8a}Budker Institute of Nuclear Physics SB RAS, Novosibirsk 630090, Russia

^{8b}Novosibirsk State University, Novosibirsk 630090, Russia

^{8c}Novosibirsk State Technical University, Novosibirsk 630092, Russia

⁹University of California at Irvine, Irvine, California 92697, USA

¹⁰University of California at Riverside, Riverside, California 92521, USA

¹¹University of California at Santa Cruz, Institute for Particle Physics, Santa Cruz, California 95064, USA

¹²California Institute of Technology, Pasadena, California 91125, USA

¹³University of Cincinnati, Cincinnati, Ohio 45221, USA

¹⁴University of Colorado, Boulder, Colorado 80309, USA

¹⁵Laboratoire Leprince-Ringuet, Ecole Polytechnique, CNRS/IN2P3, F-91128 Palaiseau, France

^{16a}INFN Sezione di Ferrara, I-44122 Ferrara, Italy

- ^{16b}*Dipartimento di Fisica e Scienze della Terra, Università di Ferrara, I-44122 Ferrara, Italy*
- ¹⁷*INFN Laboratori Nazionali di Frascati, I-00044 Frascati, Italy*
- ¹⁸*INFN Sezione di Genova, I-16146 Genova, Italy*
- ¹⁹*Indian Institute of Technology Guwahati, Guwahati, Assam 781 039, India*
- ²⁰*University of Iowa, Iowa City, Iowa 52242, USA*
- ²¹*Iowa State University, Ames, Iowa 50011, USA*
- ²²*Physics Department, Jazan University, Jazan 22822, Kingdom of Saudi Arabia*
- ²³*Johns Hopkins University, Baltimore, Maryland 21218, USA*
- ²⁴*Laboratoire de l'Accélérateur Linéaire, IN2P3/CNRS et Université Paris-Sud 11, Centre Scientifique d'Orsay, F-91898 Orsay Cedex, France*
- ²⁵*Lawrence Livermore National Laboratory, Livermore, California 94550, USA*
- ²⁶*University of Liverpool, Liverpool L69 7ZE, United Kingdom*
- ²⁷*Queen Mary, University of London, London E1 4NS, United Kingdom*
- ²⁸*University of London, Royal Holloway and Bedford New College, Egham, Surrey TW20 0EX, United Kingdom*
- ²⁹*University of Louisville, Louisville, Kentucky 40292, USA*
- ³⁰*Johannes Gutenberg-Universität Mainz, Institut für Kernphysik, D-55099 Mainz, Germany*
- ³¹*University of Manchester, Manchester M13 9PL, United Kingdom*
- ³²*University of Maryland, College Park, Maryland 20742, USA*
- ³³*Massachusetts Institute of Technology, Laboratory for Nuclear Science, Cambridge, Massachusetts 02139, USA*
- ³⁴*McGill University, Montréal, Québec, Canada H3A 2T8*
- ^{35a}*INFN Sezione di Milano, I-20133 Milano, Italy*
- ^{35b}*Dipartimento di Fisica, Università di Milano, I-20133 Milano, Italy*
- ³⁶*University of Mississippi, University, Mississippi 38677, USA*
- ³⁷*Université de Montréal, Physique des Particules, Montréal, Québec, Canada H3C 3J7*
- ³⁸*INFN Sezione di Napoli and Dipartimento di Scienze Fisiche, Università di Napoli Federico II, I-80126 Napoli, Italy*
- ³⁹*NIKHEF, National Institute for Nuclear Physics and High Energy Physics, NL-1009 DB Amsterdam, The Netherlands*
- ⁴⁰*University of Notre Dame, Notre Dame, Indiana 46556, USA*
- ⁴¹*Ohio State University, Columbus, Ohio 43210, USA*
- ^{42a}*INFN Sezione di Padova, I-35131 Padova, Italy*
- ^{42b}*Dipartimento di Fisica, Università di Padova, I-35131 Padova, Italy*
- ⁴³*Laboratoire de Physique Nucléaire et de Hautes Energies, IN2P3/CNRS, Université Pierre et Marie Curie-Paris6, Université Denis Diderot-Paris7, F-75252 Paris, France*
- ^{44a}*INFN Sezione di Perugia, I-06123 Perugia, Italy*
- ^{44b}*Dipartimento di Fisica, Università di Perugia, I-06123 Perugia, Italy*
- ^{45a}*INFN Sezione di Pisa, I-56127 Pisa, Italy*
- ^{45b}*Dipartimento di Fisica, Università di Pisa, I-56127 Pisa, Italy*
- ^{45c}*Scuola Normale Superiore di Pisa, I-56127 Pisa, Italy*
- ⁴⁶*Princeton University, Princeton, New Jersey 08544, USA*
- ^{47a}*INFN Sezione di Roma, I-00185 Roma, Italy*
- ^{47b}*Dipartimento di Fisica, Università di Roma La Sapienza, I-00185 Roma, Italy*
- ⁴⁸*Universität Rostock, D-18051 Rostock, Germany*
- ⁴⁹*Rutherford Appleton Laboratory, Chilton, Didcot, Oxon OX11 0QX, United Kingdom*
- ⁵⁰*CEA, Irfu, SPP, Centre de Saclay, F-91191 Gif-sur-Yvette, France*
- ⁵¹*SLAC National Accelerator Laboratory, Stanford, California 94309, USA*
- ⁵²*University of South Carolina, Columbia, South Carolina 29208, USA*
- ⁵³*Southern Methodist University, Dallas, Texas 75275, USA*
- ⁵⁴*Stanford University, Stanford, California 94305, USA*
- ⁵⁵*State University of New York, Albany, New York 12222, USA*
- ⁵⁶*Tel Aviv University, School of Physics and Astronomy, Tel Aviv 69978, Israel*
- ⁵⁷*University of Tennessee, Knoxville, Tennessee 37996, USA*
- ⁵⁸*University of Texas at Austin, Austin, Texas 78712, USA*
- ⁵⁹*University of Texas at Dallas, Richardson, Texas 75083, USA*
- ^{60a}*INFN Sezione di Torino, I-10125 Torino, Italy*
- ^{60b}*Dipartimento di Fisica, Università di Torino, I-10125 Torino, Italy*
- ⁶¹*INFN Sezione di Trieste and Dipartimento di Fisica, Università di Trieste, I-34127 Trieste, Italy*
- ⁶²*IFIC, Universitat de Valencia-CSIC, E-46071 Valencia, Spain*

⁶³*University of Victoria, Victoria, British Columbia, Canada V8W 3P6*⁶⁴*Department of Physics, University of Warwick, Coventry CV4 7AL, United Kingdom*⁶⁵*University of Wisconsin, Madison, Wisconsin 53706, USA*

(Received 14 June 2016; published 19 July 2016)

Many models of physics beyond the standard model predict the existence of new Abelian forces with new gauge bosons mediating interactions between “dark sectors” and the standard model. We report a search for a dark boson Z' coupling only to the second and third generations of leptons in the reaction $e^+e^- \rightarrow \mu^+\mu^-Z'$, $Z' \rightarrow \mu^+\mu^-$ using 514 fb⁻¹ of data collected by the *BABAR* experiment. No significant signal is observed for Z' masses in the range 0.212–10 GeV. Limits on the coupling parameter g' as low as 7×10^{-4} are derived, leading to improvements in the bounds compared to those previously derived from neutrino experiments.

DOI: [10.1103/PhysRevD.94.011102](https://doi.org/10.1103/PhysRevD.94.011102)

In spite of the many successes of the standard model (SM), the known particles and interactions are insufficient to explain cosmological and astrophysical observations of dark matter. This motivates the possibility of new hidden sectors that are only feebly coupled to the SM; by analogy with the SM, such sectors may contain their own interactions with new gauge bosons (Z'). In the simplest case of a hidden U(1) interaction, SM fields may directly couple to the Z' , or alternatively the Z' boson may mix with the SM hypercharge boson, which typically results from an off-diagonal kinetic term [1]. In the latter case, the Z' inherits couplings proportional to the SM gauge couplings; due to large couplings to electrons and light-flavor quarks, such scenarios are strongly constrained by existing searches [2–8].

When SM fields are directly charged under the dark force, however, the Z' may interact preferentially with heavy-flavor leptons, greatly reducing the sensitivity of current searches. Such interactions could account for the experimentally measured value of the muon anomalous magnetic dipole moment [9], as well as the discrepancy in the proton radius extracted from measurements of the Lamb shift in muonic hydrogen compared to observations in nonmuonic atoms [10,11]. Direct Z' couplings to left-handed leptons also lead to new interactions involving SM neutrinos that increase the cosmological abundance of sterile neutrinos mixing with SM neutrinos, consistent with the observed dark matter abundance [12].

We report herein a search for dark bosons Z' with vector couplings only to the second and third generations of leptons [13,14] in the reaction $e^+e^- \rightarrow \mu^+\mu^-Z'$, $Z' \rightarrow \mu^+\mu^-$. While such a scenario can be additionally constrained by

neutrino-nucleus scattering at neutrino beam experiments, the measurement presented here is also sensitive to models where couplings to neutrinos are absent, such as a gauge boson coupled exclusively to right-handed muons [15]. This search is based on 514 fb⁻¹ of data collected by the *BABAR* detector at the PEP-II e^+e^- storage ring, mostly taken at the $\Upsilon(4S)$ resonance, but also at the $\Upsilon(3S)$ and $\Upsilon(2S)$ peaks, as well as in the vicinity of these resonances [16]. The *BABAR* detector is described in detail elsewhere [17,18]. Dark boson masses between the dimuon threshold and 10 GeV are probed [19]. To avoid experimental bias, the data are only examined after finalizing the analysis strategy. A sample of about 5% of the data set is used to optimize and validate the analysis strategy, and is then discarded.

Signal events are simulated by MadGraph 5 [20] and hadronized in Pythia 6 [21] for Z' mass hypotheses ranging from the dimuon mass threshold to 10.3 GeV. The background arises mainly from QED processes. The $e^+e^- \rightarrow \mu^+\mu^-\mu^+\mu^-$ reaction is generated with Diag36 [22], which includes the full set of lowest order diagrams, while the $e^+e^- \rightarrow \mu^+\mu^-(\gamma)$ and $e^+e^- \rightarrow \tau^+\tau^-(\gamma)$ processes are simulated with KK [23]. Other sources of background include $e^+e^- \rightarrow q\bar{q}$ ($q = u, d, s, c$) continuum production, simulated with JETSET [24], and $e^+e^- \rightarrow \pi^+\pi^-J/\psi$ events, generated using EvtGen [25] with a phase-space model. The detector acceptance and reconstruction efficiencies are determined using a Monte Carlo (MC) simulation based on GEANT4 [26].

We select events containing two pairs of oppositely-charged tracks, where both positively-charged or both negatively-charged tracks are identified as muons by particle identification algorithms (PID). Identifying only two muons maintains high signal efficiency while rejecting almost all background sources but $e^+e^- \rightarrow \mu^+\mu^-\mu^+\mu^-$ events. In addition, the sum of energies of electromagnetic clusters above 30 MeV not associated to any track must be less than 200 MeV to remove background containing neutral particles. To suppress background from the decay chain $\Upsilon(3S, 2S) \rightarrow \pi^+\pi^-\Upsilon(1S)$, $\Upsilon(1S) \rightarrow \mu^+\mu^-$, we reject events taken on the $\Upsilon(2S)$ or $\Upsilon(3S)$ peaks containing any

*Present address: Wuhan University, Wuhan 43072, China.

†Present address: Università di Bologna and INFN Sezione di Bologna, I-47921 Rimini, Italy.

‡Present address: University of Huddersfield, Huddersfield HD1 3DH, UK.

§Present address: University of South Alabama, Mobile, Alabama 36688, USA.

¶Also at: Università di Sassari, I-07100 Sassari, Italy.

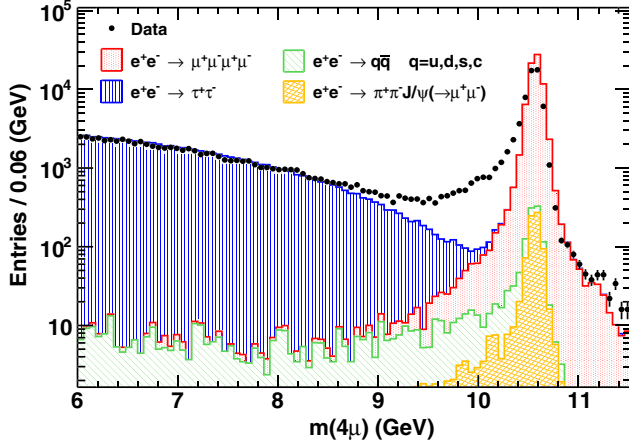


FIG. 1. The distribution of the four-muon invariant mass, $m(4\mu)$, for data taken at the $\Upsilon(4S)$ peak together with Monte Carlo predictions of various processes normalized to data luminosity. The $e^+e^- \rightarrow \mu^+\mu^-\mu^+\mu^-$ Monte Carlo does not include ISR corrections.

pair of oppositely charged tracks with any dimuon invariant mass within 100 MeV of the nominal $\Upsilon(1S)$ mass.

The distribution of the four-muon invariant mass after these cuts is shown in Fig. 1 for the data taken at the $\Upsilon(4S)$ center-of-mass (CM) energy. The background at low masses is fairly well reproduced by the simulation, while the $e^+e^- \rightarrow \mu^+\mu^-\mu^+\mu^-$ Monte Carlo overestimates the full-energy peak by $\sim 30\%$ and fails to reproduce the radiative tail. This is expected, since Diag36 does not simulate initial state radiation (ISR). We further select $e^+e^- \rightarrow \mu^+\mu^-\mu^+\mu^-$ events by requiring a four-muon invariant mass within 500 MeV of the nominal CM energy, allowing for the possibility of ISR emission. The four-muon system is finally fitted, constraining its CM energy to be within the beam energy spread and the tracks to originate from the interaction point to within its uncertainty. This kinematic fit is solely used to improve the Z' mass resolution of the bulk of events near the full-energy peak; no further requirement is imposed on the fit quality. We do not attempt to select a single $Z' \rightarrow \mu^+\mu^-$ candidate per event, but simply consider all combinations.

The distribution of the reduced dimuon mass, $m_R = \sqrt{m_{\mu^+\mu^-}^2 - 4m_\mu^2}$, is shown in Fig. 2, together with the predictions of various Monte Carlo simulations. The reduced mass has a smoother behavior near threshold and is easier to model than the dimuon mass. The spectrum is dominated by $e^+e^- \rightarrow \mu^+\mu^-\mu^+\mu^-$ production, with additional contributions from $e^+e^- \rightarrow \pi^+\pi^-\rho$, $\rho \rightarrow \pi^+\pi^-$, $e^+e^- \rightarrow \mu^+\mu^-\rho$, $\rho \rightarrow \pi^+\pi^-$, and $e^+e^- \rightarrow \pi^+\pi^-J/\psi$, $J/\psi \rightarrow \mu^+\mu^-$ events, where one or several pions are misidentified as muons. A peak corresponding to the ρ meson is visible at low mass; the second Z' candidate reconstructed in these events generates the enhancement

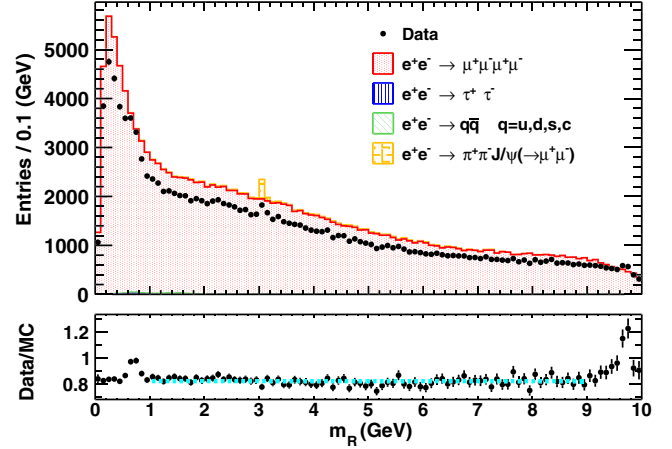


FIG. 2. The distribution of the reduced dimuon mass, m_R , together with Monte Carlo predictions of various processes normalized to data luminosity. Four combinations per event are included. The fit of the ratio between reconstructed and simulated events is shown as a light blue dashed line. The $e^+e^- \rightarrow \mu^+\mu^-\mu^+\mu^-$ Monte Carlo does not include ISR or other efficiency corrections (see text).

near 9.5 GeV. Other than the J/ψ , no significant signal of other narrow resonances is observed.

The signal efficiency rises from $\sim 35\%$ at low masses to $\sim 50\%$ around $m_R = 6-7$ GeV, before dropping again at higher masses. The signal efficiencies include a correction factor of 0.82, which primarily accounts for the impact of ISR not included in the simulation, as well as differences between data and simulation in trigger efficiency, charged particle identification, and track and photon reconstruction efficiencies. This correction factor is derived from the ratio of the m_R distribution in simulated $e^+e^- \rightarrow \mu^+\mu^-\mu^+\mu^-$ events to the observed distribution in the mass region 1–9 GeV, excluding the J/ψ region (light blue line in Fig. 2). An uncertainty of 5% is propagated as a systematic uncertainty, covering the small variations between data-taking periods and the uncertainties on the $e^+e^- \rightarrow \mu^+\mu^-\mu^+\mu^-$ cross-section.

We extract the signal yield as a function of $m_{Z'}$ by performing a series of unbinned maximum likelihood fits to the reduced dimuon mass spectrum, covering the mass range $m_R < 10$ GeV for the data taken near the $\Upsilon(4S)$ resonance, and up to 9 GeV for the data sets collected near the $\Upsilon(2S)$ and $\Upsilon(3S)$ resonances. The search is conducted in varying mass steps that correspond to the dark boson mass resolution. Each fit is performed over an interval 50 times broader than the signal resolution at that mass for $m_R > 0.2$ GeV, or over a fixed interval 0–0.3 GeV for $m_R < 0.2$ GeV. We estimate the signal resolution by Gaussian fits to several simulated Z' samples for the purpose of determining the scan steps, and interpolate the results to all other masses. The resolution varies between 1–9 MeV, dominated by experimental effects. We probe a total of 2219 mass hypotheses. The bias in the

fitted values, estimated from a large ensemble of pseudoexperiments, is negligible.

The likelihood function, described below, contains components from signal, continuum background, and peaking background where appropriate. The signal probability density function (pdf) is modeled directly from the signal Monte Carlo mass distribution using a nonparametric kernel density function. The pdf is interpolated between the known simulated masses using an algorithm based on the cumulative density function [27]. An uncertainty of 0.1–3.2 events associated to this procedure is estimated by taking the next-to-closest mass point in place of the closest simulated mass point to interpolate the signal shape. The agreement between the simulated signal resolution and the data is assessed by fitting the full-energy peak of the four-muon invariant mass spectrum in the range 10.3–10.7 GeV with a Crystal Ball function [28]. The ratio of simulated and reconstructed peak widths is 1.01 ± 0.04 , consistent with unity. The impact of ISR emission on the peak widths are expected to be small in that mass range. Similarly, the decay width of the J/ψ resonance is well reproduced by the simulation within its uncertainty.

The background is described by a function of the form $\arctan(ax + bx^2 + cx^3)$ for fits in the low mass region, where a , b , c are free parameters, and by a second order polynomial above $m_R = 0.2$ GeV. The two methods give similar signal yields at the transition point. Peaking contributions from the J/ψ resonance are modeled from the mass distribution extracted from the corresponding Monte Carlo, leaving the yield as a free parameter. We exclude the resonant region from the search, vetoing a range of ± 30 MeV around the nominal J/ψ mass. The contribution from ρ -meson decay is very wide and easily absorbed by the background fit in each narrow window. We estimate the uncertainty associated with the background model by repeating the fit using a third order polynomial in the high-mass region or a fourth-order polynomial constrained to pass through the origin in the low mass range. This uncertainty is as large as 35% of the statistical uncertainty in the vicinity of the dimuon threshold and high-mass boundary, but remains at a level of a few percent outside these regions.

The $e^+e^- \rightarrow \mu^+\mu^-Z'$, $Z' \rightarrow \mu^+\mu^-$ cross section is extracted for each data set as a function of the Z' mass by dividing the signal yield by the efficiency and luminosity. The uncertainties on the luminosity (0.6%) [16] and the limited Monte Carlo statistics (1–3%) are propagated as systematic uncertainties. The cross sections are finally combined and displayed in Fig. 3. We consider all but the uncertainties on the luminosity and the efficiency corrections to be uncorrelated. The statistical significance of each fit is taken as $\mathcal{S}_S = \text{sign}(N_{\text{sig}}) \sqrt{2 \log(\mathcal{L}/\mathcal{L}_0)}$, where N_{sig} is the fitted signal yield, and \mathcal{L} (\mathcal{L}_0) is the maximum likelihood values for a fit including (excluding) a signal. These significances are almost Gaussian, and the combined

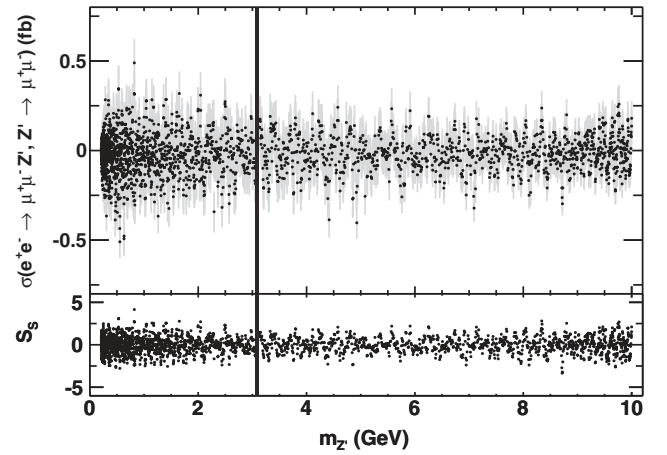


FIG. 3. The measured $e^+e^- \rightarrow \mu^+\mu^-Z'$, $Z' \rightarrow \mu^+\mu^-$ cross section together with its statistical significance, \mathcal{S}_S (see text for definition), as a function of the Z' mass. The uncertainty on each point is shown as light gray error bars. The dark gray band indicates the region excluded from the analysis.

significance is derived under this assumption. A large sample of Monte Carlo experiments is generated to estimate trial factors. The largest local significance is 4.3σ , observed near $m_{Z'} = 0.82$ GeV, corresponding to a global significance of 1.6σ , consistent with the null hypothesis.

We derive 90% confidence level (CL) Bayesian upper limits (UL) on the cross-section $\sigma(e^+e^- \rightarrow \mu^+\mu^-Z'$, $Z' \rightarrow \mu^+\mu^-)$, assuming a uniform prior in the cross section by integrating the likelihood from zero up to 90% of its area. Correlated (uncorrelated) systematic uncertainties are included by convolving the combined (individual) likelihood with Gaussian distributions having variances equal to the corresponding uncertainties. The results are displayed in Fig. 4 as a function of the Z' mass. The

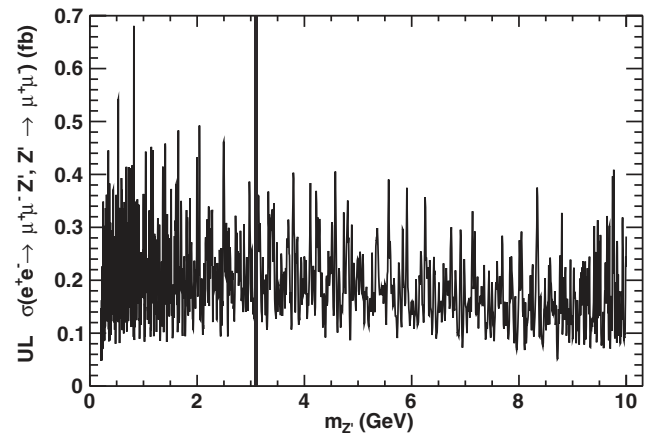


FIG. 4. The 90% CL upper limits on the cross section $\sigma(e^+e^- \rightarrow \mu^+\mu^-Z'$, $Z' \rightarrow \mu^+\mu^-)$ as a function of the Z' mass. The dark gray band indicates the region excluded from the analysis.

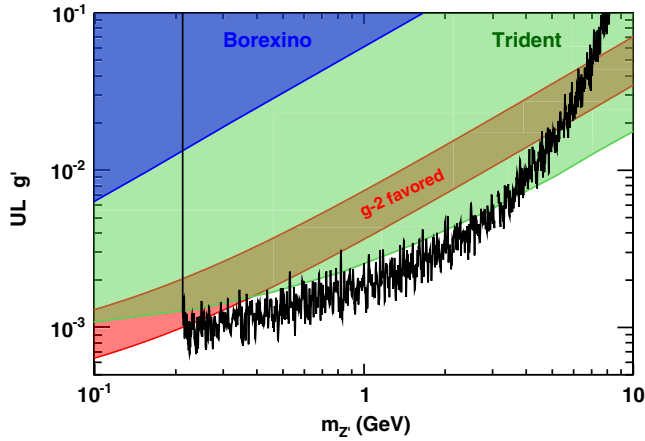


FIG. 5. The 90% CL upper limits on the new gauge coupling g' as a function of the Z' mass, together with the constraints derived from the production of a $\mu^+\mu^-$ pair in ν_μ scattering (“Trident” production) [29,30]. The region consistent with the discrepancy between the calculated and measured anomalous magnetic moment of the muon within 2σ is shaded in red.

corresponding 90% CL upper limits on the coupling parameter g' in the scenario with equal magnitude vector couplings to muons, taus, and the corresponding neutrinos are shown in Fig. 5, together with constraints derived from neutrino experiments [29]. Upper limits down to 7×10^{-4} near the dimuon threshold are set.

In summary, we report the first search for the direct production of a new muonic dark force boson, providing a model-independent test of theories with new light particles coupled to muons. For identical coupling strength to muons, taus, and the corresponding neutrinos, we exclude all but a sliver of the remaining parameter space preferred

by the discrepancy between the calculated and measured anomalous magnetic moment of the muon above the dimuon threshold [29], and we set the strongest bounds for nearly all of the parameter space below ~ 3 GeV. Because this search relies only on the Z' coupling to muons, the result can also be interpreted giving powerful constraints on other new vectors and scalars that interact exclusively with muons.

We thank Maxim Pospelov for helpful conversations. We are grateful for the extraordinary contributions of our PEP-II2 colleagues in achieving the excellent luminosity and machine conditions that have made this work possible. The success of this project also relies critically on the expertise and dedication of the computing organizations that support *BABAR*. The collaborating institutions wish to thank SLAC for its support and the kind hospitality extended to them. This work is supported by the US Department of Energy and National Science Foundation, the Natural Sciences and Engineering Research Council (Canada), the Commissariat à l’Energie Atomique and Institut National de Physique Nucléaire et de Physique des Particules (France), the Bundesministerium für Bildung und Forschung and Deutsche Forschungsgemeinschaft (Germany), the Istituto Nazionale di Fisica Nucleare (Italy), the Foundation for Fundamental Research on Matter (The Netherlands), the Research Council of Norway, the Ministry of Education and Science of the Russian Federation, Ministerio de Economía y Competitividad (Spain), the Science and Technology Facilities Council (United Kingdom), and the Binational Science Foundation (U.S.-Israel). Individuals have received support from the Marie-Curie IEF program (European Union) and the A. P. Sloan Foundation (USA).

-
- [1] B. Holdom, *Phys. Lett.* **166B**, 196 (1986).
 - [2] R. Essig *et al.*, arXiv:1311.0029, and references therein.
 - [3] D. Babusci *et al.* (KLOE-2 Collaboration), *Phys. Lett. B* **736**, 459 (2014).
 - [4] H. Merkel *et al.* (A1 Collaboration), *Phys. Rev. Lett.* **112**, 221802 (2014).
 - [5] J. P. Lees *et al.* (*BABAR* Collaboration), *Phys. Rev. Lett.* **113**, 201801 (2014).
 - [6] J. R. Batley *et al.* (NA48/2 Collaboration), *Phys. Lett. B* **746**, 178 (2015).
 - [7] A. Anastasi *et al.* (KLOE Collaboration), *Phys. Lett. B* **750**, 633 (2015).
 - [8] A. Anastasi *et al.* (KLOE-2 Collaboration), *Phys. Lett. B* **757**, 356 (2016).
 - [9] M. Pospelov, *Phys. Rev. D* **80**, 095002 (2009).
 - [10] V. Barger, C. W. Chiang, W. Y. Keung, and D. Marfatia, *Phys. Rev. Lett.* **106**, 153001 (2011).
 - [11] D. Tucker-Smith and I. Yavin, *Phys. Rev. D* **83**, 101702 (2011).
 - [12] B. Shuve and I. Yavin, *Phys. Rev. D* **89**, 113004 (2014).
 - [13] X.-G. He, G. C. Joshi, H. Lew, and R. R. Volkas, *Phys. Rev. D* **43**, R22 (1991).
 - [14] X.-G. He, G. C. Joshi, H. Lew, and R. R. Volkas, *Phys. Rev. D* **44**, 2118 (1991).
 - [15] B. Batell, D. McKeen, and M. Pospelov, *Phys. Rev. Lett.* **107**, 011803 (2011).
 - [16] J. P. Lees *et al.* (*BABAR* Collaboration), *Nucl. Instrum. Methods Phys. Res., Sect. A* **726**, 203 (2013).
 - [17] B. Aubert *et al.* (*BABAR* Collaboration), *Nucl. Instrum. Methods Phys. Res., Sect. A* **479**, 1 (2002).
 - [18] B. Aubert *et al.* (*BABAR* Collaboration), *Nucl. Instrum. Methods Phys. Res., Sect. A* **729**, 615 (2013).
 - [19] Natural units ($\hbar = c = 1$) are used throughout this paper.

- [20] J. Alwall, R. Frederix, S. Frixione, V. Hirschi, F. Maltoni, O. Mattelaer, H.-S. Shao, T. Stelzer, P. Torrielli, and M. Zaro, *J. High Energy Phys.* **07** (2014) 079.
- [21] T. Sjostrand, S. Mrenna, and P. Z. Skands, *J. High Energy Phys.* **05** (2006) 026.
- [22] F. A. Berends, P. H. Daverveldt, and R. Kleiss, *Nucl. Phys.* **B253**, 441 (1985).
- [23] S. Jadach, B. F. L. Ward, and Z. Was, *Phys. Rev. D* **63**, 113009 (2001).
- [24] T. Sjostrand, *Comput. Phys. Commun.* **82**, 74 (1994).
- [25] D. J. Lange, *Nucl. Instrum. Methods Phys. Res., Sect. A* **462**, 152 (2001).
- [26] S. Agostinelli *et al.* (GEANT4 Collaboration), *Nucl. Instrum. Methods Phys. Res., Sect. A* **506**, 250 (2003).
- [27] A. L. Read, *Nucl. Instrum. Methods Phys. Res., Sect. A* **425**, 357 (1999).
- [28] T. Skwarnicki, Ph.D. thesis, Institute of Nuclear Physics, Cracow, 1986; DESY Report No. DESY F31-86-02, Appendix E.
- [29] W. Altmannshofer, S. Gori, M. Pospelov, and I. Yavin, *Phys. Rev. Lett.* **113**, 091801 (2014).
- [30] A. Kamada and H. B. Yu, *Phys. Rev. D* **92**, 113004 (2015).